Hindawi
Wireless Communications and Mobile Computing
Volume 2022, Article ID 9945908, 8 pages
https://doi.org/10.1155/2022/9945908

Research Article

FDD LTE Performance Simulation Based on Massive Antenna Array

Jun Wang [1] and Dejun Mu [2,3]

[1]*School of Automation, Northwestern Polytechnical University, Xi'an 710000, China*
[2]*School of Cybersecurity, Northwestern Polytechnical University, Xi'an 710000, China*
[3]*Research & Development Institute of Northwestern Polytechnical University, Shenzhen 518057, China*

Correspondence should be addressed to Jun Wang; 648051693@qq.com

Received 24 May 2022; Revised 20 June 2022; Accepted 24 June 2022; Published 4 July 2022

Academic Editor: Kuruva Lakshmanna

Copyright © 2022 Jun Wang and Dejun Mu. This is an open access article distributed under the Creative Commons Attribution License, which permits unrestricted use, distribution, and reproduction in any medium, provided the original work is properly cited.

There are two methodologies to realize 3D MIMO for FDD LTE, MU-MIMO-based virtual beam (VB), and four-cell soft-split cell (SSC), which beamforms four logical cells in one physical sector, and this paper is aimed at figuring out which brings more performance between VB and SSC. In the first place, brief introduction for the mechanism of VB and SSC are presented. Subsequently, detailed systematic simulations based on WINNER II are carried out based on different traffic models (low load, medium load, and high load) and user distribution is also considered. For accurate evaluation on the performance gain of VB and SSC, 4T4R solution is also simulated as the benchmark, which is widely deployed to improve the capacity of FDD LTE by operators. Based on the simulation of results of the subsequent KPIs, cell throughput, average cell throughput, average UE throughput, and average layer number, VB and SSC effectively increase single-cell capacity and user experience in high load scenario compared with 4T3S solution and VB can bring more gain.

1. Introduction

LTE will still be dominant at 49.9% of all global mobile subscriptions with 5G accounting for 39.4% of the global market by the end of 2026 [1]. Meantime, the existing LTE spectrum, such as B3, B28, is evolved to satisfy the cover layer of 5G network. Undoubtedly, this will decrease the capacity of LTE in a live network sharply, especially in dense urban. Therefore, how to increase the single-cell capacity of LTE with existing spectrum is a critical issue in hotspot areas for global operators.

3D MIMO is an effective technique to improve the spectral efficiency and the single-cell capacity for both frequency division duplex (FDD) LTE and time division duplex (TDD) LTE which utilizes massive antenna array to realize beamforming [2–4]. To fully utilize the benefits of massive antenna array, accurate channel state information (CSI) are required to achieve high beamforming gains. While acquiring these channels in TDD LTE is an easy task due to the channel reciprocity and 3D MIMO is firstly deployed in live network, such a property does not apply to FDD LTE setup where the uplink and downlink channels are totally different [5], and the realization of 3D MIMO for FDD LTE is still studied and is focused in this article.

Massive MIMO antenna array is the key of 3D MIMO and is normally plate-like linear array with 16/32/64/96 elements. By adjusting the phase of each element, the time difference caused by different paths of signals sent from different array elements can be compensated and the in-phase superposition of signals in the expected direction can be maximized. Once the signal direction changes, the maximum direction of the antenna beam can be changed correspondingly through the phase shift to realize beam scanning and tracking. By using this feature, the incoming direction estimation of FDD system can be evaluated, that is, direction of arrival (DOA) [6] estimation, which lays a foundation for channel estimation. 32 transmitters and 32 receivers (32T32R) is mainly applied in live FDD LTE network and is focused in this article.

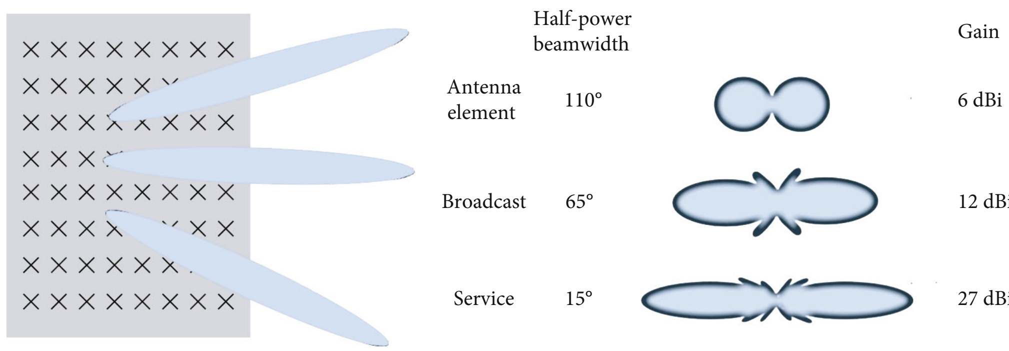

Figure 1: Massive antenna array.

There are two methodologies to realize 3D MIMO: virtual beam (VB) and soft-split cell (SSC). Virtual beam adapts MU-MIMO technology to realize beamforming both in horizontal and vertical directions, while soft-split beam utilizes beamforming to split four logical cells in horizontal direction. Here, simple introductions for VB and SSC are showed in this article. In the meantime, detailed capacity estimation also is presented based on systematic simulation on virtual beam and SSC from the perspective of downlink (DL) cell throughput and average user throughput.

2. Methodology of VB and SSC

Massive antenna array can effectively realize 3D MIMO technology to increase single-cell capacity and the number of antennas varies from 16 to 128 [7]. In spatial modulation, the number of antennas is also critical because it represents the spatial state number of the modulation. Massive antenna array with 32 antennas for FDD LTE was commercially proposed by ZTE and HUAWEI in 2016 and are being improved to satisfy commercial deployment. Undoubtedly, 3D MIMO based on 32T32R is our focus.

Massive antenna array is formed by antenna elements in a certain way. In other words, the vector field generated by antenna elements is superimposed to massive antenna array and the current amplitude and phase distribution on element antennas should meet the appropriate relationship. Based on these features, massive antenna can easily realize narrow beam to improve antenna direction and gain, beamforming, phase scanning of beam, and low side-lobe pattern. As showed in Figure 1, massive antenna array system for FDD LTE is 32T32R with $2\,(\text{vertical}) * 8\,(\text{horizontal}) * 2\,(\text{dual polarization})$, the gain of antenna element is 6 dBi with the half-power beam width of 110°, the gain of broadcast is 12 dBi with the half-power beam width of 65°, and the gain of service can reach 27 dBi with the half-power beam width of 15°.

Massive antenna array based on 3D MIMO can provide not only azimuth beam to cover the horizontal but also elevation beam to cover the vertical, which can effectively improve space multiplexing. Meanwhile, massive antenna array can provide extremely narrow beam through beamforming, which can suppress interference.

Massive MIMO is one of massive antenna array-based technologies that utilizes beamforming, beam tracking, SDMA, or MU-MIMO to enable multiple users to occupy identical time and frequency resources simultaneously. CSI is essential for the realization of channel equalization, user detection, precoding, and other technologies. For FDD LTE, since the uplink and downlink channels adopt different frequencies and the fading conditions experienced by the uplink and downlink channels are different, the downlink CSI needs to be obtained through user equipment (UE) feedback. After each user estimates the downlink channel information according to the downlink training sequence, it is fed back to the base station through vector quantization channel. TM3/4 channel estimation adopts cell-specific reference signal (CRS), UE feedbacks rank indicator (RI), and precoding matrix indicator (PMI) according to CRS, and eNodeB (eNB) selects codebook for data transmission. UE data demodulation still adopts CRS, so it is unable to carry out flexible beam orientation. Channel state information reference signal (CSI-RS) is used for TM9 channel estimation, and UE-level demodulation reference signal (DM-RS) is used for data demodulation, which is sent together with user data. The same precoding is used to support beamforming and automatically track the user's azimuth. To realize tracking, we first need to know which direction the user's signal comes from. This is DOA estimation. The base station side requires the user to send mutually orthogonal uplink reference signals. The signals received by different antennas are only different in phase. The DOA can be estimated based on the phase difference and antenna distance.

As showed in Figure 2, massive MIMO provides both azimuth beam and elevation beam based on UE location and there are eight narrow beams for both azimuth and elevation simultaneously.

Figure 3 shows another 3D MIMO technology based on massive antenna array, SSC. It utilizes beamforming to form 4 wide beams and each beam is one independent logical cell-like normal cell.

3. Simulation Principle and Key Definition

The first step for systematic simulation is to choose the 3D channel model. So far, the evaluation and standardization techniques of 3D MIMO techniques in 3GPP have been primarily based on 3D channel models from SCM, ITU,

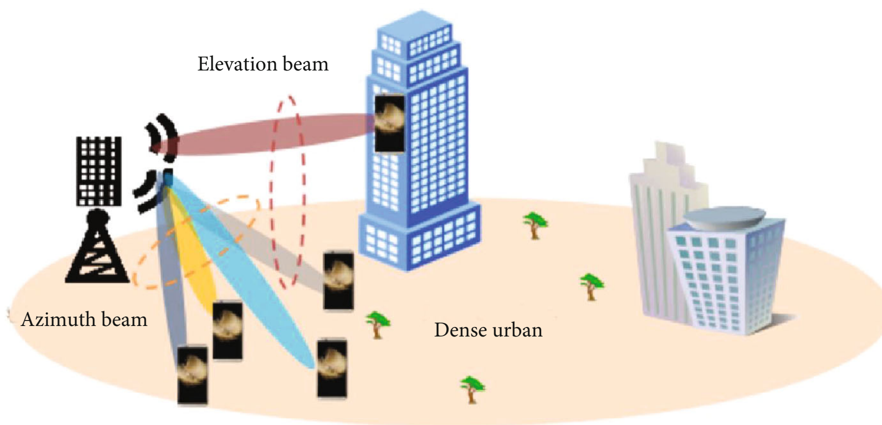

Figure 2: Massive antenna array for VB.

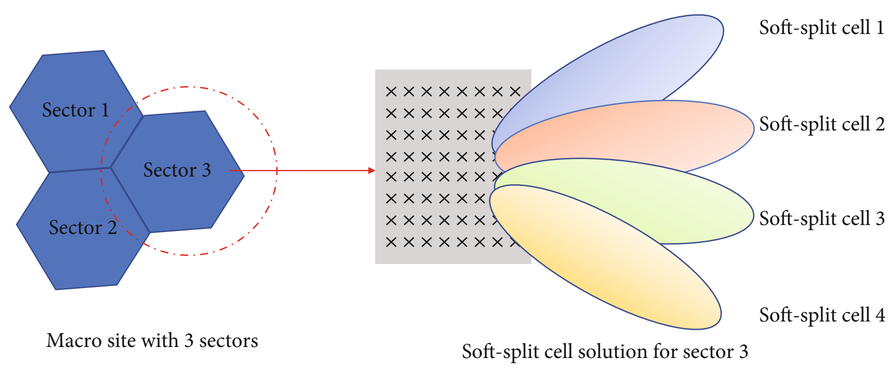

Figure 3: Massive antenna array for SSC.

and WINNER II [8, 9]. The 3D channel model of WINNER II can be effectively satisfy simulation requirements because antenna parameters and channel parameters are relatively independent. Therefore, the 3D channel model of WINNER II is chosen for our simulation [10].

Application environments also should be considered. Undoubtedly, 3D MIMO technology should be used in high load area and most areas are in dense urban. Urban macro (3D-Uma) with enhanced eNBs located outdoors are considered to be typical usage scenario for 3D MIMO and densely populated by buildings and homogeneous in nature. The value of key parameters are set as showed in Table 1.

UE distribution in cell also may cause the capacity changes in live FDD LTE network, and uniform and non-uniform UE distribution are also considered as showed in Figure 4.

The traffic model in live network also impacts the capacity, and three types of traffic model are defined based on scheduled UE per time transmission interval (TTI) and transport block size (TBS) as in Table 2 [11]. The principle of traffic model is as follows:

(1) Bit denotes transmission block allocated to each user per TTI

(2) 1000 bits has the probability to occupy all 50 PRBs even with $MCS = 0$ ($I_{TBS} = 0$) in Table 3, so its low load and packet are almost discontinuous

(3) 5400 bits has the partial probability to occupy all 50 PRBs with $MCS > 7$ ($ITBS = 7$) in Table 3, so its medium low load and packet are always continuous

(4) 150000 bits is always to occupy all 50 PRBs even with $MCS = 28$ ($I_{TBS} = 26$) in Table 3 so its high load and packet are always full buffer

In [12], 4T4R can significantly improve capacity and user experience compared with 2T2R and is widely deployed in live FDD LTE network. Therefore, 4T4R is a baseline to measure the capacity gain of VB and SSC. The simulation parameter set of macro site with 3 4T4R sectors (4T3S) is as showed in Table 4. Considering most UEs only have 2 receivers and support TM4 in live network, as mentioned in [12], the transmission mode is set to be TM4 and the UE receiver number is also set to 2.

In live FDD LTE network, DL average MCS, average cell throughput, average user throughput, and PRB ratio are used as key performance indicators (KPIs) to measure the performance of eNB as mentioned in [12], and the above

Table 1: Key parameter set for virtual beam and SSC.

Parameter configuration	Value set
Network topology	1 site with 3 sectors
UL/DL frequency	1940 MHz/2130 MHz
Average active user number per sector	60
Transmission mode	TM4
CRS port number configuration	CRS 4 port
Reference signal (RS) energy per resource element (EPRS)	15 dBm
System bandwidth	10 MHz
Simulation model	3D-UMa NLOS
Massive antenna array system	32T32R
SSC	4 soft-split cell in horizontal direction
VB	MU-MIMO

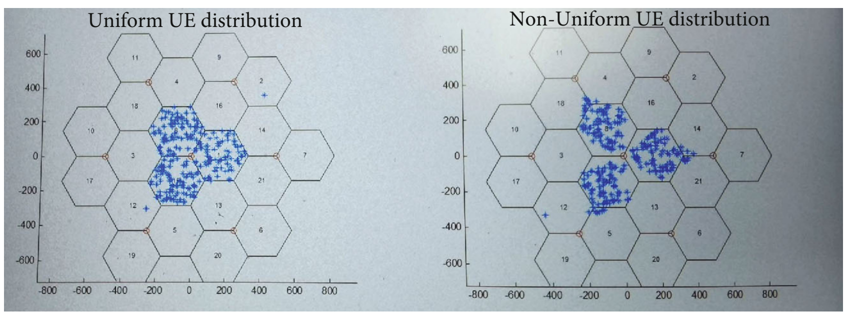

Figure 4: Uniform and nonuniform UE distribution for UE.

Table 2: Simulation traffic model.

Traffic model	Load	Scheduled UE no./TTI	Bit (TBS/ UE)
Small and discontinuous packet	Low	2	1000
Large and continuous packet	Medium	3	5400
Full buffer traffic	High	60	15000

Table 3: From <7.1.7.2.1 transport blocks not mapped to two-layer spatial multiplexing> of TS36.213.

	43	44	45	46	47	48	49	50
0	1192	1224	1256	1256	1288	1320	1352	1384
1	1544	1608	1608	1672	1736	1736	1800	1800
2	1928	1992	2024	2088	2088	2152	2216	2216
3	2536	2536	2600	2664	2728	2792	2856	2856
4	3112	3112	3240	3240	3368	3496	3496	3624
5	3752	3880	4008	4008	4136	4264	4392	4392
6	4584	4584	4776	4776	4968	4968	5160	5160
7	5352	5352	5544	5736	5736	5992	5992	6200
25	27376	28336	28336	29296	29296	30576	31704	31704
26	31704	32856	32856	34008	35160	35160	36696	36696

KPIs are also used to measure the performance of VB and SSC in this paper. In addition, the average layer number is also KPI for VB and SSC:

(1) DL average MCS: DL average MCS is defined as follows:

$$\text{DLAvgMCS} = \frac{\sum_0^{28} i * \text{NumMCSi}}{\sum_0^{28} \text{NumMCSi}}, \quad (1)$$

where NumMCSi is the scheduling number of MCS = i in all considering TTI.

(2) Average cell throughput: DL cell throughput is defined as follows:

$$\text{CellTHP} = \frac{\text{TotalPDCPVol}}{\text{SchTime}}, \quad (2)$$

where TotalPDCPVol is the total PDCP SDU data volume transferred in a cell with considering all TTIs [7]. SchTime is a counter. It counts the duration from the time data appears in the downlink service buffer to the time the service buffer comes empty in a measurement period of all eNBs and sampling period is 1 ms.

Table 4: Key parameter set 4T3S.

Parameter configuration	Value set
Network topology	1 site with 3 sectors
UL/DL frequency	1940 MHz/2130 MHz
Average active user number per sector	60
Transmission mode	TM4
CRS port number configuration	CRS 4 port
Reference signal (RS) energy per resource element (EPRS)	15 dBm
System bandwidth	10 MHz
Simulation model	2D-UMa NLOS

Table 5: Low load, small packet, and discontinuous packet.

	Uniform UE distribution			Nonuniform UE distribution		
	4T3S	VB	SSC	4T3S	VB	SSC
Average cell THP (mbps)	5.29	5.36	6.03	5.55	5.68	6.33
Average cell traffic (Gbit/H)	19.03	19.31	21.71	19.98	20.46	22.79
Average UE THP (mbps)	0.09	0.09	0.10	0.11	0.11	0.11
Average MCS	21.21	21.52	21.46	21.81	22.20	22.81
Average layer number	1.0	1.00	1.00	1.00	1.00	1.00
Average PRB ratio (%)	22	5	6	20	5	6

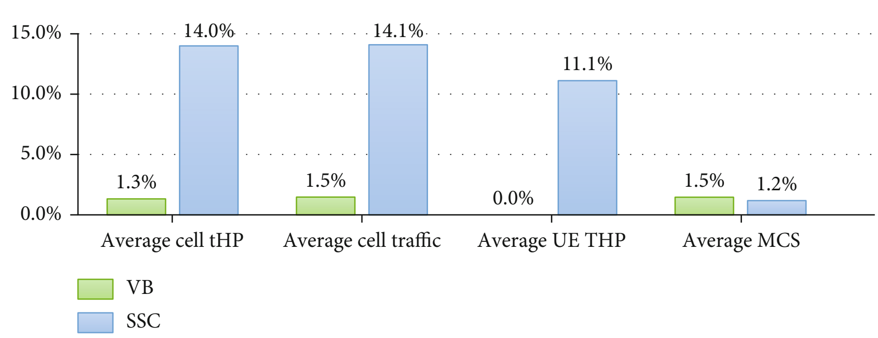

Figure 5: Gain ratio of VB and SSC compared to 4T3S in traffic mode with low load and uniform user distribution.

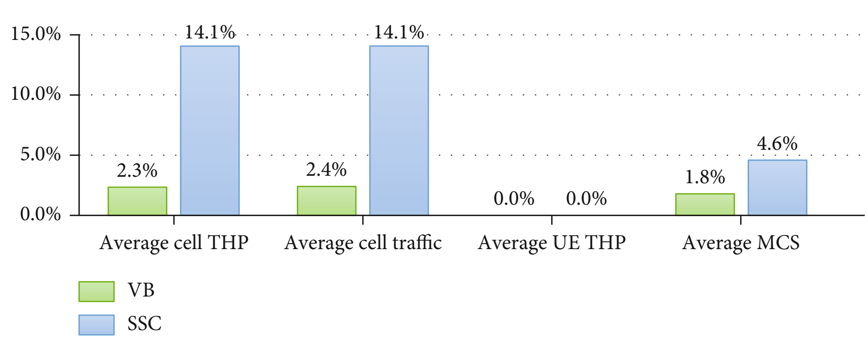

Figure 6: Gain ratio of VB and SSC compared to 4T3S in traffic mode with low load and nonuniform user distribution.

Table 6: Medium load, medium packet, and almost-continuous packet.

	Uniform UE distribution			Nonuniform UE distribution		
	4T3S	VB	SSC	4T3S	VB	SSC
Average cell THP (mbps)	19.6	21.31	20.10	19.99	21.38	21.21
Average cell traffic (Gbit/H)	70.58	76.72	72.36	71.95	76.97	76.36
Average UE THP (mbps)	0.34	0.37	0.35	0.38	0.41	0.39
Average MCS	17.02	16.93	16.87	16.83	17.55	17.32
Average layer number	1.00	1.16	1.08	1.00	1.09	1.05
Average PRB ratio (%)	92	24	27	86	22	26

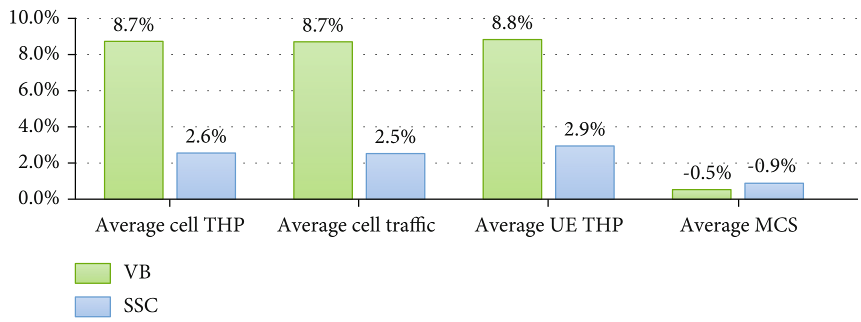

Figure 7: Gain ratio of VB and SSC compared to 4T3S in traffic mode with medium load and uniform user distribution.

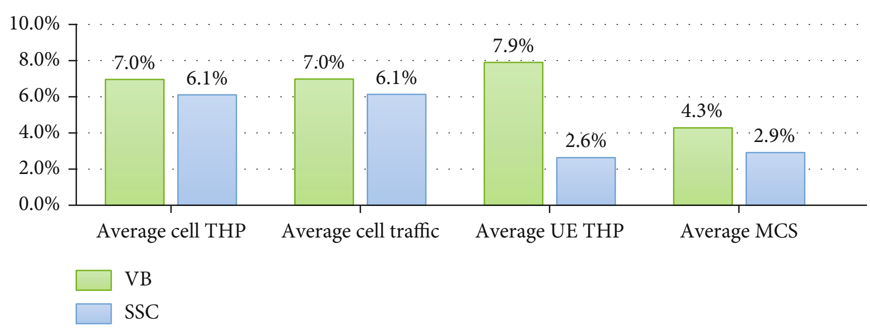

Figure 8: Gain ratio of VB and SSC compared to 4T3S in traffic mode with medium load and nonuniform user distribution.

(3) Average user throughput: average user throughput is defined as follows:

$$\text{AvgUTHP} = \frac{\text{TotalPDCPU}}{\text{USchTime}}, \quad (3)$$

where TotalPDCPU is the total downlink PDCP SDU dead load, not including packets lost at the UE interface, tail packets, and data completed through one data scheduling, and counter USchTime counts the downlink service time during which eNB buffer becomes empty from being not empty, not including the data transmission time for tail packets and data competed through one data scheduling.

4. Result Analysis

Table 5 shows the simulation results of traffic model with low load. In both uniform UE distribution and nonuniform UE distribution, the average cell throughput of SSC increased by 14% compared with as that of 4T3S while the average cell throughput is almost the same as 4T3S in Figures 5 and 6. In addition, the performance trend is the same both in uniform UE distribution and nonuniform UE distribution.

Table 6 shows the simulation results of traffic model with medium load. In both uniform UE distribution and nonuniform UE distribution, the VB performance is better than SSC. However, the gain of average cell THP of VB is less than 10% compared with that of 4T3S in Figures 7 and 8. The average PRB ratio of 4T3S exceeds 86%, but the average

Table 7: High load, full buffer, and continuous packet.

	Uniform UE distribution			Nonuniform UE distribution		
	4T3S	VB	SSC	4T3S	VB	SSC
Average cell THP (mbps)	25.78	50.78	47.03	30.25	54.02	49.16
Average cell traffic (Gbit/H)	92.80	182.80	169.31	108.90	194.46	176.98
Average UE THP (mbps)	0.44	0.87	0.81	0.58	1.03	0.85
Average MCS	18.29	14.38	11.77	19.01	16.32	10.21
Average layer number	1.00	2.45	4.00	1.00	2.05	4.00
Average PRB ratio (%)	99	64	99	99	51	99

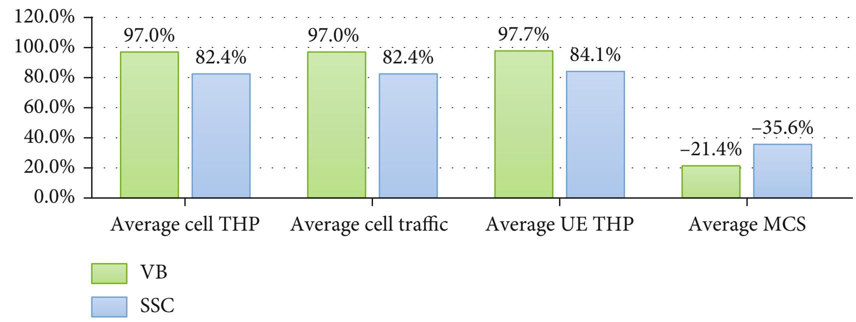

Figure 9: Gain ratio of VB and SSC compared to 4T3S in traffic mode with high load and uniform user distribution.

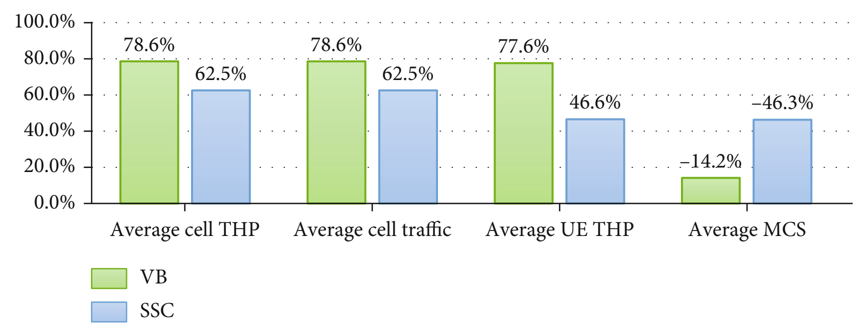

Figure 10: Gain ratio of VB and SSC compared to 4T3S in traffic mode with high load and nonuniform user distribution.

PRB ratio of VB and SSC is less than 30%. In other words, the capacity of 4T3S almost reaches its maximum capability.

Table 7 shows the simulation results of traffic model with high load. In traffic model with high load, cell capacity and average UE THP of both VB and SSC are obviously and sharply increased compared with 4T3S, which reaches its maximum capability.

Figure 9 shows the performance gain of VB and SSC with uniform UE distribution:

For average cell THP, the average cell THP of VB reaches 50.78 mbps with 64% PRB ratio while the average cell THP of SSC reaches 47.03 mbps with 99% PRB ratio. However, the average cell THP of VB still can be improved with 36% unused PRB.

For perspective of average MCS, with the increase of service, the MCS degradation of SSC is more severe than VB although the MCS degradation of VB is still more severe than 4T3S. In other words, in terms of the capability of interference suppress, VB is better than SSC.

Figure 10 shows the performance gain of VB and SSC with nonuniform UE distribution; the performance characteristic is the same with uniform UE distribution.

Based on the analysis on the above results, the following conclusions can be given compared to 4T3S solution:

(1) The performance gain trend of VB and SSC is same in the scenarios of low load, medium load, and high load in the situation of both uniform UE distribution and nonuniform distribution

(2) The performance gain of VB and SSC is slight compared to 4T3S solution in the scenarios of low load and high load

(3) The performance gain of VB and SSC is obvious in high load. In the scenarios of uniform UE distribution, for average cell THP, the average cell THP of VB reaches 50.78 mbps with 64% PRB ratio while the average cell THP of SSC reaches 47.03 mbps with

99% PRB ratio. However, the average cell THP of VB still can be improved with 36% unused PRB

(4) In high load, the performance gain in uniform UE distribution is more obvious than that in nonuniform UE distribution. Therefore, the UE distribution also will affect the performance of VB and SSC

(5) In high load, the performance gain of VB is better than SSC in both uniform UE distribution and nonuniform UE distribution, especially the PRB utilization of VB is sharply lower than SSC. In the other hand, the average MCS of SSC is also lower than VB, which shows the interference of SSC is severer than VB

5. Conclusion and Future Work

Both MU-MIMO based VB and four-cell based SSC obviously and sharply improve cell capacity and user experience for high-load cell compared to 4T3S in FDD LTE network, and the performance of VB is slightly better than SSC because of PRB utilization and interference suppressing.

In the meantime, there are still some limitations and challenges. First of all, MU-MIMO-based VB has the potential to further improve performance and four-cell-based SSC needs to optimize the mechanism of interference suppressing. Secondly, our simulation is based on site level while cluster level should be simulated. More importantly, both VB and SSC should be verified in live FDD LTE network.

Data Availability

The datasets used and/or analyzed during the current study are available from the corresponding author on reasonable request.

Conflicts of Interest

Both authors declare no potential conflicts of interest with respect to the research, authorship, and/or publication of this article.

References

[1] "GSA, LTE & 5G subscribers – Update|March|2022," 2022.

[2] 3GPP, RP-122034, "Study on 3D-channel model for elevation beamforming and FD-MIMO studies for LTE, RAN#58," 2012.

[3] 3GPP, "TR 36.873 V12.7.0, Study on 3D channel model for LTE," 2017.

[4] 3GPP, "TR 25.996 V16.0.0, Spatial channel model for multiple input multiple output (MIMO) simulations," 2020.

[5] J. Chen, X. Zhang, and P. Zhang, "DDL-based sparse channel representation and estimation for downlink FDD massive MIMO systems," in *2020 IEEE International Conference on Communications, ICC 2020*, pp. 1–6, Dublin, Ireland, 2020.

[6] H. Huang, J. Yang, H. Huang, Y. Song, and G. Gui, "Deep learning for super-resolution channel estimation and DOA estimation based massive MIMO system," *IEEE Transactions on Vehicular Technology*, vol. 67, no. 9, pp. 8549–8560, 2018.

[7] P. Pajusco, F. Gallée, N. Malhouroux, and R. Burghelea, "Massive antenna array for space-time channel sounding," in *2017 11th European Conference on Antennas and Propagation (EUCAP)*, pp. 865–868, Paris, France, 2017.

[8] "ITU-R M.2135-1, Guidelines for evaluation of radio interface technologies for IMT-advanced," 2009.

[9] "WINNER II channel models, deliverable D1.1.2 V1.2, IST-4-027756 WINNER II deliverable," 2008.

[10] B. Mondal, T. Thomas, E. Visotsky et al., "3D channel model in 3GPP," *IEEE Communications Magazine*, vol. 53, no. 3, pp. 16–23, 2015.

[11] 3GPP, "TS 36.213 V12.8.0, evolved universal terrestrial radio access (E-UTRA): physical layer procedures," 2012.

[12] J. Wang and M. Dejun, "4T4R performance analysis in live FDD LTE network," in *Modern Industrial IoT, Big Data and Supply Chain*, vol. 218, pp. 75–81, Springer, Singapore.